Low Cycle Fatigue Behaviour of an Al–Li Alloy

N. ESWARA PRASAD*, G. MALAKONDAIAH*,
K. N. RAJU** and P. RAMA RAO*

**Defence Metallurgical Research Laboratory, P.O. Kanchanbagh, Hyderabad-500 258, India*

***National Aeronautical Laboratory, Bangalore, India*

ABSTRACT

The low cycle fatigue behaviour of a commercial Al-Li alloy 8090 has been studied in the as-received (T851) condition in both longitudinal and long-transverse directions. The material exhibits cyclic stability at lower strain amplitudes and cyclic softening at higher strain amplitudes. The cyclic strain hardening coefficient (n') is seen to vary with strain amplitude and the alloy exhibits two stage cyclic work hardening behaviour. The fatigue life - plastic strain data display a bilinear nature of Coffin - Manson plots. Fractographic analysis indicates change in fracture mode with applied strain amplitude. These observations provide a possible explanation for the observed transition in terms of change in both deformation mechanism as well as fracture modes.

KEYWORDS

Low cycle fatigue; Al-Li alloy 8090; Cyclic stress response; Coffin-Manson plots; Fractography.

INTRODUCTION

Low cycle fatigue (LCF) studies in precipitation hardening aircraft aluminium alloys have been extensively carried out and have provided valuable information [Calabrese and Laird, 1974, 1977; Kuhlmann-Wilsdorf and Laird, 1977, 1979] not only about the LCF characteristics of these alloys but also in terms of structure-property relationships. Thus LCF work on the new class of aircraft structural alloys based on the Al-Li system is naturally attractive and gaining ground. Dhers et al. [1986] have pointed out that lithium in solid solution causes negligible effect on cyclic deformation behaviour. On the other hand, Srivatsan et al. [1986] showed in the case of a low Li, high Cu aluminium alloy 2020 that unrecrystallised microstructure exhibits considerable improvement in fatigue resistance as compared to the recrystallised microstructure. We report here the results obtained on LCF behaviour of a commercial Al-Li alloy 8090.

II. EXPERIMENTAL

The aluminium - lithium quaternary alloy 8090 was obtained from Alcan, England in T851 condition in the form of 12.5 mm thick plate. LCF tests were conducted on specimens oriented parallel to the longitudinal (L) as well as long - transverse (LT) directions. Cylindrical specimens of 15 mm parallel length and 6.5 mm gauge diameter were used. Mechanically polished specimens were finally chemical polished in a solution containing, by vol. pct., 70 H_3PO_4, 25 H_2SO_4 and 5 HNO_3 at 343 K to obtain a surface finish better than 0.1 μm.

Fully - reversed, total strain controlled LCF tests were conducted at room temperature in laboratory air atmosphere on a computer controlled servohydraulic MTS 880 testing system. The test frequency was maintained at 0.1 Hz. The data recorded for each test include the peak tensile and compressive stress amplitudes, stress range ($\Delta\sigma$) and plastic strain amplitude ($\Delta\epsilon_p$) as a function of elapsed cycles. The failure limit was set at 20% drop in peak stress range or complete separation. Tensile tests were conducted using LCF specimen geometry at a strain rate of 3×10^{-3} s^{-1}. A 10 mm extensometer was used to monitor the strain.

III. RESULTS AND DISCUSSION

Microstructure

The optical micrograph of the alloy in the as-received condition (Fig.1) reveals elongated pan-cake structure with partial recrystallization. The average grain width is 5 - 9 μm, with a large grain aspect ratio. The microstructure consists of dense and uniform Al_3Li (δ', the strengthening phase) and Al_2CuMg (S', the phase causing slip homogenisation) [White et al., 1986], which features can be observed only at higher resolutions.

Cyclic Stress Response

The cyclic stress response of the alloy in longitudinal and long-transverse directions is shown in Fig.2. A moderate cyclic hardening is seen in the first few cycles. Following hardening, the material at low strain amplitudes attains cyclic stability which is maintained nearly upto fracture. On the other hand, at higher strain amplitudes the alloy exhibits considerable softening. The trend is seen to be the same for both the directions although there is a disparity in the critical strain amplitudes, beyond which softening sets in ($\Delta\epsilon_p/2 = 1.5 \times 10^{-3}$ for L direction; $\Delta\epsilon_p/2 = 1.2 \times 10^{-3}$ for L-T direction).

Following the earlier work [Srivatsan and Coyne, 1986], cyclic softening beyond a critical strain amplitude can be understood in terms of repeated shearing of precipitates giving rise to localised deformation by precipitate dissolution [Abel and Ham, 1966], over-aging [Lynch and Ryder, 1973] or precipitate disordering [Sanders et al., 1977].

Cyclic Stress - Strain Behaviour

Cyclic stress-strain curves corresponding to longitudinal and long-transverse directions are shown in Fig.3. For the sake of comparison, tensile stress-strain curves are also included. Cyclic as well as monotonic data were analysed in terms of the power-law relationships, namely

$$(\Delta\sigma/2) = K' (\Delta\epsilon_p/2)^{n'} \quad ..1a$$

$$\sigma = K (\epsilon_p)^n \quad ..1b$$

where $\Delta\sigma/2$ and $\Delta\epsilon_p/2$ are the cyclic stress and plastic strain amplitudes at half-life; σ and ϵ_p are the true stress and true plastic strains; K' and K are the cyclic and monotonic strength coefficients and n' and n are cyclic and monotonic work hardening exponents respectively. The parameters thus derived are listed in Tables I and II. The analysis reveals that in both the cases, a single power-law relation describes the monotonic stress-strain behaviour. On the other hand, n' is seen to exhibit two stage cyclic work hardening behaviour (Fig.3). In both the test directions, n' at lower strain amplitudes has a higher value as compared to that at higher strain amplitudes.

Fatigue Life

The Coffin-Manson (C-M) plots corresponding to longitudinal and long-transverse directions are shown in Figs. 4 and 5. Plastic strain amplitude ($\Delta\epsilon_p/2$) at half-life is plotted against number of reversals to failure ($2N_f$). In both the cases the Coffin-Manson plots are bilinear in nature, showing a transition. The fatigue life variation with plastic strain amplitude in hypo- as well as hyper-transitional regions can be expressed in terms of the C-M relationship,

$$(\Delta\epsilon_p/2) = \epsilon_f' (2N_f)^c \quad ..2$$

where ϵ_f' and c are fatigue ductility coefficient and fatigue ductility exponent respectively. The extrapolation of the hypo-transition region of C-M plots to $N_f = 1/2$, yields ϵ_f', which matches well with the tensile ductility. The values obtained for ϵ_f' and c are listed in Table II.

Fatigue life data are further analysed in terms of total strain amplitude ($\Delta\epsilon_t/2$) expressed as the sum of elastic ($\Delta\epsilon_e/2$) and plastic ($\Delta\epsilon_p/2$) strain components,

$$\Delta\epsilon_t/2 = \Delta\epsilon_e/2 + \Delta\epsilon_p/2 = \frac{\sigma_f'}{E}(2N_f)^b + \epsilon_f'(2N_f)^c \quad ..3$$

where σ_f' and b are fatigue strength coefficient and fatigue strength exponent respectively and E is the elastic modulus. The constant σ_f' and b can be obtained from the fatigue life and cyclic stress amplitude data, using the equation

$$(\Delta\sigma/2) = \sigma_f' (2N_f)^b \quad ..4$$

The fatigue life parameters thus derived are included in Table II. The cyclic constant K' and n' can also be estimated from fatigue strength and ductility parameters as $K' = \sigma_f'/(\epsilon_f')^{n'}$ and $n' = b/c$. The values of K' and n' thus obtained for L direction are seen (Table II) to be in good agreement with those derived from cyclic stress-strain data (Eq. 1a) and differ considerably in case of L-T direction. Fatigue constants thus evaluated are found to be of similar magnitude as those reported for other commercial aluminium alloys [Sanders and Starke, 1977] and Al-Li alloys [Srivatsan et al., 1986].

A transition in Coffin-Manson curves has been observed in several other materials [Dhers et al., 1986; Feng et al., 1984; Srivatsan et al., 1986]. The earlier reports on fatigue life data of Al-Li alloys also suggest a transition at a plastic strain amplitude of about 10^{-3} as observed in the present work (Figs. 4 and 5). Interestingly the transition strain values obtained from Eq. 2 nearly correspond to the values of the test strain amplitudes below which cyclic stress response is stable and above which stress response curves show cyclic softening (Figs. 2,4 & 5). Various mechanisms have been proposed

to explain the non-ideal C-M relationship. One possibility is the change in fracture morphology with increasing strain amplitude [Coffin, 1971]. Alternatively there could be a change in deformation behaviour essentially through work hardening characteristics [Mediratta et al., 1986] and likewise of slip homogeneity [Sanders et al., 1977]. Yet another possibility is environment assisted fatigue degradation [Coffin, 1972; Sanders and Starke, 1976]. Either of the above mechanisms or in combination should explain the bilinear nature of C-M relationship. As stated earlier, the transition in C-M plots corresponds to a change in the nature of material's cyclic stress response (i.e., whether the response suggests the stress stability or softening) and also cyclic work hardening behaviour. Both the observations point to the possibility of a change in the deformation mechanism with increasing strain amplitude. The transition in n' associated with bilinear C-M plots observed in the present study is in line with the findings on dual phase steels by Mediratta et al. [1986]. However, the deduced transition strains do not correspond well in constrast to the observations of Mediratta et al.. In both directions, the transition strains corresponding to n' are seen to be considerably lower as compared to those in C-M relationship (Figs. 3,4 & 5). Contrary to these observations, very recently Srivatsan [1988] reported a single n' in case of an Al alloy 2020 though the C-M plots reflect bilinear nature. Detailed microscopic studies at higher resolutions are therefore needed to clearly establish whether a change in the deformation behaviour with increasing strain amplitudes has occured and if so, of what extent. Fractographic studies have revealed that the change in the slope of C-M plots also corresponds to a change in fracture mode.

Fracture surfaces were examined under an ISI 100A scanning electron microscope to see the possibility of a change in fracture mode with increasing strain amlitude. Figures 4 and 5 include the fractographs showing the fracture features of the specimens tested in L and L-T directions at various strain amplitudes. These fractographs clearly depict a gradual change in fracture mode. With increase in strain amplitude, the fracture mode appears to change from a higher energy transgranular shear or slip band fracture (Figs. 4a, b and 5a, b) to a lower energy ductile intergranular fracture (Figs. 4e - g and 5e - h). Localised plastic deformation due to particle shearing results in intergranular fracture at higher strain amplitudes. The fractographs corresponding to the transition region show mixed morphology indicating features of both the types of fracture (Figs. 4c, d and 5c,d). The bilinear nature of C-M plots observed in the present study can thus be related to a change in fracture mode.

Fatigue behaviour of Al-Li alloy 8090 observed in the present study is compared in Fig.6 with that of other aluminium alloys, namely Al-Li alloy 2020 [Srivatsan et al., 1986], RR58 [Malakondaiah and Rama Rao, 1977], 2024-T4 and 7075-T6 [Endo and Morrow, 1969] at matching strength levels excepting for the 7075 alloy which shows higher yield strength (680 MPa). The Al-Li alloys 8090 and 2020 evidently posses matching fatigue resistance in hypo-transitional region. On the other hand, in the hyper-transition region, the alloy 2020 exhibits superior fatigue performance as compared to the alloy 8090. The alloy RR58 appears to be the best in low cycle fatigue. At any given strain amplitude, the fatigue life of RR58 is more than an order of magnitude higher than that of Al-Li alloys. The fatigue resistance of the alloys 2024 and 7075 is seen to be intermediate.

CONCLUSIONS

1. The alloy in both the directions exhibits cyclic stability at lower strain amplitudes and cyclic softening at higher strain amplitudes. The change in cyclic stress behaviour occurs at a plastic strain amplitude 1.5 x 10^{-3} in L direction and 1.2 x 10^{-3} in L-T direction.
2. Over the entire strain range investigated, irrespective of the test direction, the alloy is characterised by a single n. On the other hand, n' is seen to vary with strain amplitude. The value of n' is found to be higher at lower strain amplitudes as compared to that at higher strain amplitudes.
3. Fatigue life data for both the directions show a transition in Coffin-Manson plots. The transition strains match well with those corresponding to the change in material's cyclic stress response stated in (1) above and differ considerably with the transition strains pertaining to n'. The transition strains corresponding to n' are nearly an order of magnitude lower as compared to those in C-M plots.
4. Fractographic studies reveal change in the fracture mode; low energy fracture features, like ductile intergranular were observed above the transition strain and at strains lower than the transition, fracture surfaces were characterised by a higher energy fracture, like transgranular shear or slip band fracture. Around the transition strain, fracture features are mixed.
5. When compared with other aluminium alloys, the Al-Li alloys possess similar fatigue resistance at lower strain levels. On the other hand, at higher strain amplitudes the Al-Li alloys are inferior in LCF to the Al-Cu-Mg and Al-Zn-Mg alloys.

ACKNOWLEDGEMENTS

The authors are thankful to Shri G. Sundara Sarma and Shri D.V.V.Satyanarayana for their help in carrying out the fractographic studies.

REFERENCES

Abel, A and Ham, R.K (1966), Acta Met., 14, p.1495.
Calabrese, C and Laird, C (1974), Mater. Sci. Engg., 13, p.141; 159.
Chen, R.T and Starke, E.A (1984), Mater. Sci. Engg., 67, p.229
Coffin, L.F (1971), J. Metals, 6,p.388.
Coffin, L.F (1972), Met. Trans., 3A, p.1777.
Dhers, J, Driver, J and Fourdeux, A (1986), in 'Aluminium - Lithium Alloys III', ed. Baker, C, Gregson, P.J, Harris, S.J and Peel, C.J (The Institute of Metals, London), p.233.
Endo, T and Morrow, JoDean (1969), J. Metals, 4, p.159.
Feng, W.X, Lin, F.S and Starke, E.A (1984), Met. Trans., 15A, p.1209.
Kuhlmann-Wilsdorf, D and Laird, C (1977), Mater. Sci. Engg., 27, p.137.
Kuhlmann-Wilsdorf, D and Laird, C (1979), Mater. Sci. Engg., 37, p.111.
Lynch, S.P and Ryder, D.A (1973), Aluminium, 49, p.748.
Malakondaiah, G and Rama Rao, P (1977), Proc. ICF 4, p.741.
Mediratta, S.R, Ramaswamy, V and Rama Rao, P (1986), Scripta Mettal., 20, p.555.
Sanders, R.E and Starke, E.A (1977), Mater. Sci. Engg., 28, p.53.
Sanders, T.H, Mauney, D.A and Stanley, J.T (1977), in 'Fundamental Aspects of Structural Alloy Design', ed. Jaffee, R.I and Wilcox, B.A (Plenum Press, New York), p.487.
Sanders, T.H and Starke, E.A (1976),Met. Trans., 7A, p.1107.
Srivatsan, T.S (1988), Inter. J. Fatigue, 10, p.91.
Srivatsan, T.S and Coyne, E.J (1986), Inter. J. Fatigue, 8, p.201.
Srivatsan, T.S, Yamaguchi, K and Starke, E.A (1986), Mater. Sci. Engg.,

83, p.87.
White, J, Miller, W.S, Palmer, I.G, Devis, R and Saini, T.S (1986), in 'Aluminium - Lithium Alloys III', ed. Baker, C, Gregson, P.J, Harris,S.J and Peel, C.J (The Institute of Metals, London), p.530.

Table I Tensile Properties of Al-Li Alloy 8090

Direction	0.2% P.S. (MPa)	U.T.S. (MPa)	%El. (10mm gl.)	Work Hardening Coeff., n
Longitudinal	486	543	5.4	0.049
Long-Transverse	467	546	9.8	0.048

Table II Low Cycle Fatigue Parameters of Al-Li Alloy 8090

Direction	Transition Strains		Fatigue Strength Constants (Eq.4)		Fatigue Ductility Constants (Eq.2)		Constants from Fatigue Life Data		Constants from Stress Strain Data	
	in n'	in $\Delta\epsilon_p/2$	Fatigue Strength Coeff. (σ_f')	Fatigue Strength Exponent (b)	Fatigue Ductility Coeff. (ϵ_f')	Fatigue Ductility Exponent (c)	$K' = \frac{\sigma_f'}{(\epsilon_f')^{n'}}$	$n'=b/c$	K'	n'
LONGITUDINAL	2.3×10^{-4}	3.2×10^{-3}								
Hypo-Transition Region			586	0.03_5	0.05	0.42	750	0.08	870	0.09
Hyper-Transition Region			747	0.07	4.5	1.14	677	0.065	668	0.06
Long-Transverse	4.0×10^{-4}	2.6×10^{-3}								
Hypo-Transition Region			597	0.04	0.09	0.52	712	0.075	1047	0.11
Hyper-Transition Region			1170	0.12	1.94	0.96	1079	0.12	676	0.05

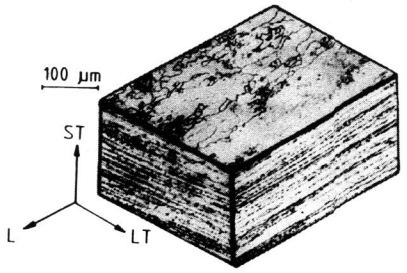

Fig.1: Triplanar optical micrograph of Al-Li alloy 8090 in T851 condition.

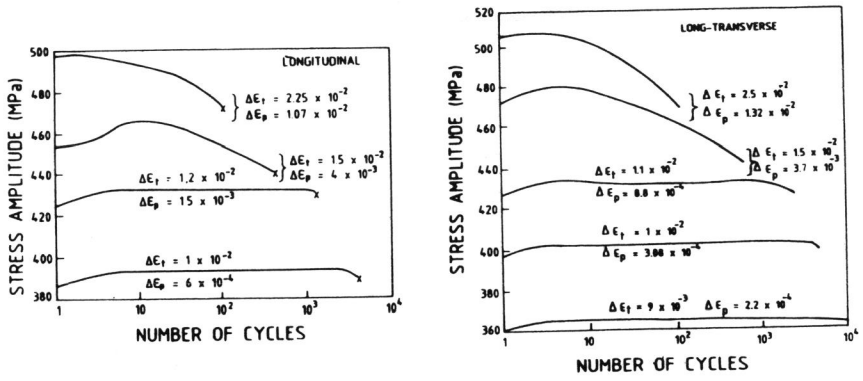

Fig.2: Cyclic stress response curves for (a) longitudinal, (b) transverse directions

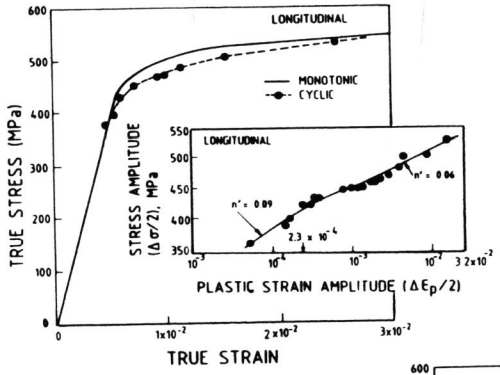

Fig.3: Cyclic as well as monatonic stress-strain curves for (a) longitudinal, (b) transverse directions.

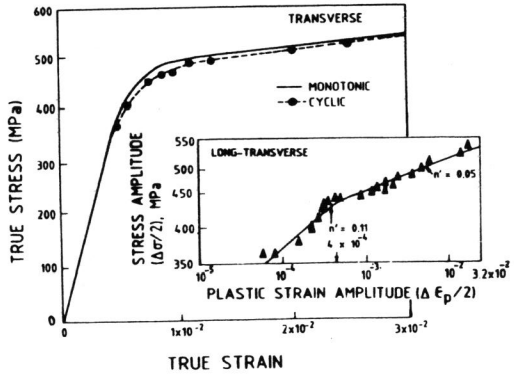

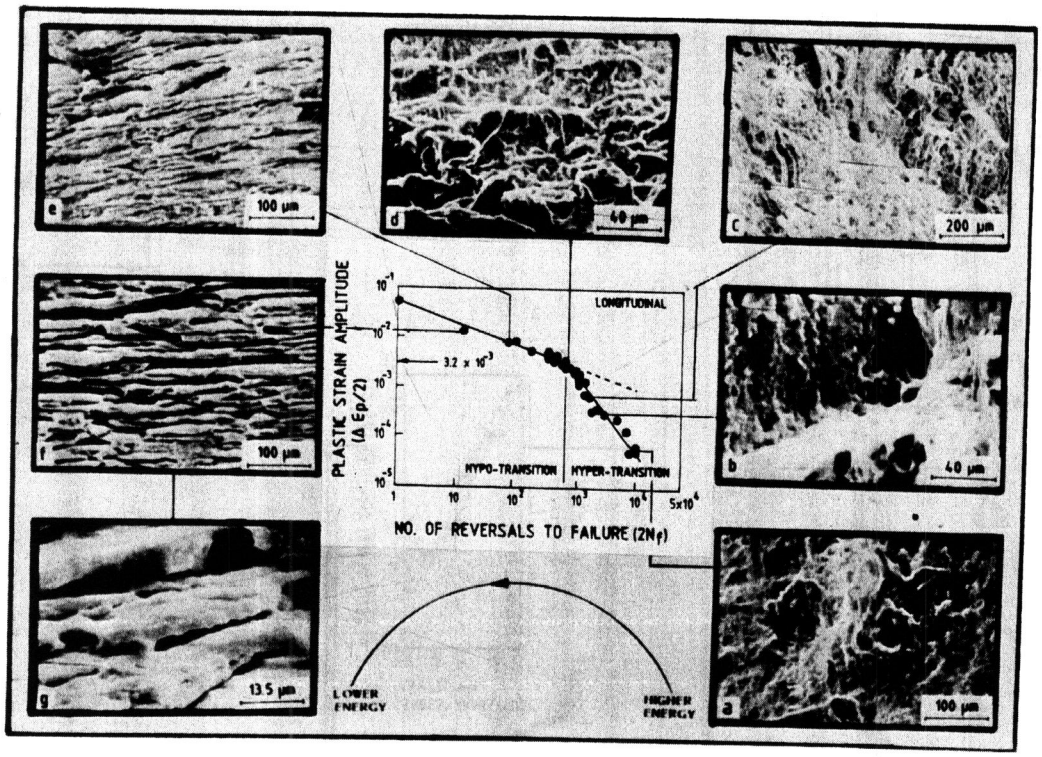

Fig.4: Coffin - Manson plot for longitudinal direction. Also included are the fractographs corresponding to plastic strain amplitudes (a) 9.5×10^{-5}, (b) 2.75×10^{-4}, (c) 6.5×10^{-4}, (d) 4.2×10^{-3}, (e) 8.55×10^{-3}, (f) 1.7×10^{-2}, (g) same as (f) at higher magnification.

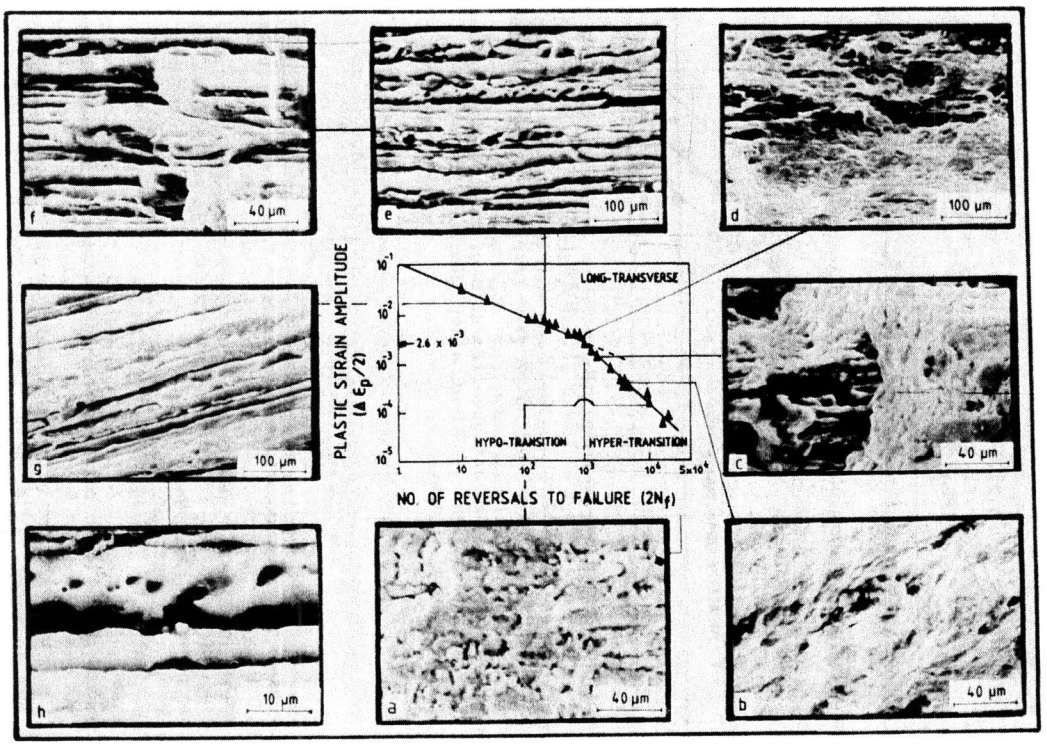

Fig.5: Coffin - Manson plot for long - transverse direction. Also included are the fractographs corresponding to plastic strain amplitudes (a) 1.2×10^{-4}, (b) 2.6×10^{-4}, (c) 1.1×10^{-3}, (d) 2.6×10^{-3}, (e) 8×10^{-3} (f) same as (e) at higher magnification, (g) 1.7×10^{-2}, (h) same as (g) at higher magnification.

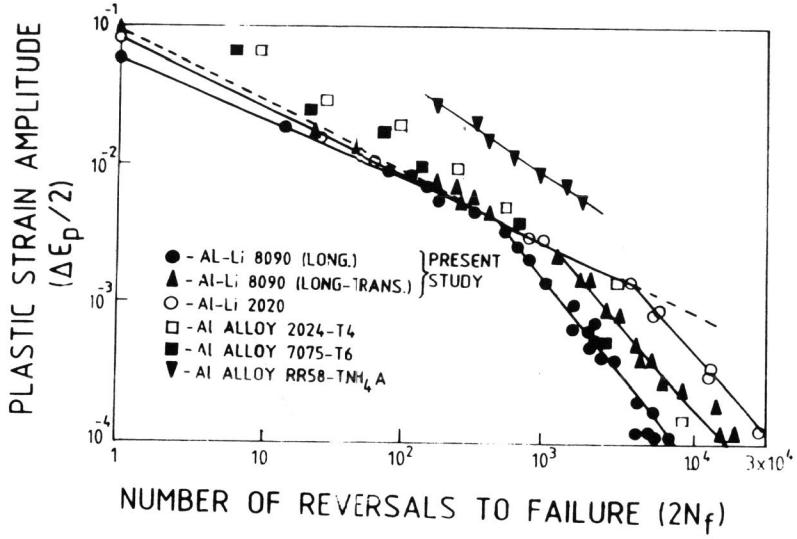

Fig.6: A comparison of fatigue life data of Al-Li alloy 8090 with that of Al-Li alloy 2020 and other aluminium alloys.